Simultaneous, Robot-Compatible γ-Ray Spectroscopy and Imaging of an Operating Nuclear Reactor

Ioannis Tsitsimpelis, Andrew West, Mauro Licata, Michael D. Aspinall, *Member, IEEE*, Anže Jazbec, Luka Snoj, *Member, IEEE*, Philip A. Martin, Barry Lennox, *Senior Member, IEEE*, and Malcolm J. Joyce, *Member, IEEE*

***Abstract*—The design and test of a robot-compatible, radiation detection instrument providing simultaneous γ-ray imaging and γ-ray spectroscopy is described. The sensing system comprises a cerium bromide inorganic scintillation detector and a cylindrical, lead slot collimator that is configured with a robot-compatible, on-board data acquisition system. The mount for the sensor is a lightweight, bespoke 3-axis gimbal actuated by servos for pan, tilt and rotation of the collimator for imaging capability. This paper discusses the integration of this relatively low-cost radiation detection apparatus with a commercially available, Robot-Operating-System-controlled robotic platform (a Clearpath Robotics™ Jackal). The detection system is compliant with the power and mass payload constraints of the robot. Its performance has been evaluated by means of two practical examples: a) measurements in a laboratory environment to assess the ability of the system to resolve two caesium-137 point sources, and b) deployment at the Jožef Stefan Institute TRIGA Mark II research reactor to assess the ability of the system to characterise the γ-ray emission at 1 kW from a horizontal tangential beam port in the reactor hall and from the reactor sample pool above the core.**

***Index Terms*— Robotics and automation, environmental monitoring and control, detection, estimation and classification based on sensor data.**

Ioannis Tsitsimpelis, Mauro Licata, Michael D. Aspinall, and Malcolm J. Joyce are with Department of Engineering, Lancaster University, Lancaster LA1 4YW, U.K. (e-mail: i.tsitsimpelis@lancaster.ac.uk; m.licata@lancaster.ac.uk; m.d.aspinall@lancaster.ac.uk; m.joyce@lancaster.ac.uk).

Andrew West and Barry Lennox are with the School of Electrical and Electronic Engineering, University of Manchester, Manchester M13 9PL, U.K. (e-mail: andrew.west@manchester.ac.uk; barry.lennox@manchester.ac.uk).

Anže Jazbec and Luka Snoj are with the Reactor Physics Division and Reactor Infrastructure Centre, Jožef Stefan Institute, SI-1000 Ljubljana, Slovenia (e-mail: anze.jazbec@ijs.si; luka.snoj@ijs.si).

Philip Martin is with the Department of Chemical Engineering & Analytical Science, University of Manchester, Manchester M13 9PL, U.K. (e-mail: philip.martin@manchester.ac.uk).

Digital Object Identifier 10.1109/JSEN.2020.3035147

I. INTRODUCTION

NUCLEAR energy provides approximately 1/10th of the world's electricity from nearly 450 power plants [1]. However, radioactive materials arise from the reactors, fuel processing plants, research laboratories and waste storage facilities associated with this industry. Novel approaches to monitoring this radioactivity that reduce the need for human to be involved directly offer far-reaching benefits, such as: reducing the exposure of people to radiation, advancing the design and operational expectations of next-generation reactors, minimizing contamination risk, better safeguarding of nuclear materials and maintaining public trust. The integration of robotic systems and instrumentation focused on specific nuclear challenges has become more widespread due to advancements in the former but also due to, in the case of Fukushima, the recognition that better robotic systems are needed that are compatible with emergency response requirements [2].

This most recent wave of research and development has shown great potential thus far [3]–[8], and has been attracting the attention of stakeholders pertinent to the nuclear industry, including regulatory bodies and facilities operators. Apart from

the dedicated challenge of decommissioning the stricken reactors at Fukushima, a more universal enduring challenge, and a global touchstone when achieved, is to characterise legacy waste storage facilities; especially where human access is not possible. These challenges account for very significant levels of public expenditure ($ billions) in the UK alone, given that decommissioning these facilities is the subject of a 100- year plan [9]. The utilisation of low-cost, flexible instrumentation systems that incorporate multi-sensing capability is expected to contribute towards a reduction of the time necessary and the costs of decontamination and decommissioning activities, whilst substantiating safety margins.

The emerging use of γ-ray imaging systems has proven useful for hot-spot identification at sites such as the Fukushima Daiichi Nuclear Power Station Unit 1, particularly when deployed on robotic platforms [10]. Moreover, there are trends to incorporate these instruments more closely with their robotic platforms [11] constituting, for example, a detection system which can be operated not only by an individual worker but also directly by a robot, which may be operating autonomously: this is a critical design requirement for future sensors for remote deployment in hazardous environments.

The radiation sensing instrumentation suite presented in this article can be used as either a stand-off method to carry out radiation spectroscopy and imaging, or as a unit incorporated with a robotic platform (a Clearpath Robotics$^{\text{TM}}$ Jackal). In the guise of the latter, this extends its measurement capabilities to the benefits of mobility in places in the absence of an operator. The instrumentation is an integration of off-the-shelf and bespoke components.

The relatively low-cost instrumentation developed in this research reflects a representative prototype that applies to the needs of nuclear industry stakeholders, with regard to handling and inspecting facilities with radioactive materials. Given this trajectory, the novelty of the approach described hereafter is that day-to-day operators of such facilities can exploit this instrumentation to inspect areas of interest on a systematic or *ad hoc* basis. This has the potential to: reduce the exposure of workers to radiation; improve the clarity of information conveyed between operators and regulators; and to inform decommissioning and decontamination plans i.e., when to deploy robotic systems for these complex activities.

This article is laid out as follows. Section II provides a description of the individual subsystems that comprise the instrumentation, including their means of operation as a whole. Section III presents spectroscopy and imaging results in a laboratory setting, and from the deployment at the Jožef Stefan Institute (JSI) TRIGA Mark II reactor. Section IV discusses the overall performance of the sensing equipment and hardware, and highlights its advantages, scope for improvement and its capabilities that were not tested in this particular research. Finally, Section V presents the concluding remarks.

II. METHODS

The instrumentation developed for this research is an integration of off-the-shelf and bespoke components. It can be

Fig. 1. Integrated radiation detection instrumentation with robotic platform (side elevation, left, front, perspective view, right).

operated both in stand-alone mode and on terrestrial mobile platforms, such as the Unmanned Ground Vehicle (UGV) in this research (Fig. 1).

To achieve this, the following key requirements were satisfied: a) compliance of its mass, size, and power payload with the robot's capacities, taking into consideration additional components incorporated on it (e.g., LiDAR sensors, cameras, motors, etc.), b) that part or whole data transmission to be carried out via the Robot Operating System (ROS) interface. Compliance within the aforementioned system constraints ensures that the instrumentation does not, for example, drain the on-board battery of the robot too rapidly or occupy excess space on it, whereas provisions for ROS communication reduce the complexity of data flow and acquisition. This section provides a detailed description of the subsystems.

A. Radiation Detection Hardware and Detector

The radiation detection analysis hardware utilised for this research is a quad-channel Mixed Field Analyser (MFA, Hybrid Instruments Ltd., UK) [12]. It provides 12-bit sampling resolution at a rate of 500 MSa/s, and has neutron-γ discrimination and spectroscopic capabilities, as well as Transistor-Transistor-Logic (TTL) outputs for counting purposes [13], [14]. For this application, part of this commercial hardware has been ported into a bespoke enclosure to contain the instrumentation's electronics, with passive cooling and 12 V DC power supply. For this research, it is configured to carry out γ-ray spectroscopy via pulse gradient analysis and imaging via the TTL outputs. Its pulse shape discrimination capabilities were not used in this work.

A single, miniature cerium bromide (CeBr$_3$) scintillator (Scionix, Netherlands) [15] was used for γ-radiation detection. A small detector (in this case having a 10 mm x 10 mm crystal, see Fig. 2) was selected so that it can be deployed in-situ without occupying significant space and to yield good imaging granularity. Cerium bromide offers an effective compromise having a relatively high light output, relatively high energy resolution (between 22 %-3 % Full Width Half Maximum for energies ranging between 30 keV to 2600 keV), low intrinsic background and no need for cryogenic or mechanical cooling [16], [17].

Fig. 2.   The CeBr$_3$ detector used for this research with a UK $1 coin to indicate scale.
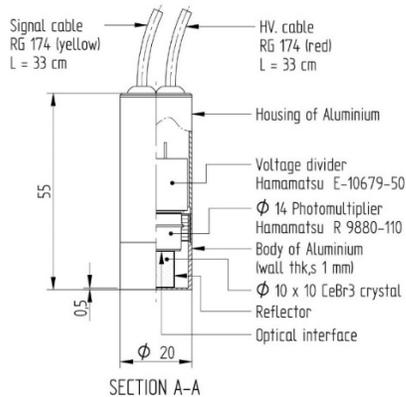

Fig. 3.   Cross-section schematic of CeBr$_3$ detector used for this research, dimensions are in mm where not indicated otherwise.

When used with the MFA, it is possible to obtain spectroscopic information of γ rays with energies up to approximately 2.5 MeV. An identical version of the detector used in this research has been tested previously on a submersible robot (AVEXIS) in tests using some of the same facilities in which it demonstrated consistent pulse height spectra calibration tests. When unshielded, irradiation tests revealed its response to be stable up to 15 Gy/h [18], [19]. As indicated by the schematic diagram of the detector in Fig. 3, the crystal is enclosed by a cylinder of 1-mm thick aluminium, of 20-mm diameter and 55-mm length, and it is coupled to a Hamamatsu R9880-110 photomultiplier tube (PMT). Two RG174 wires extending from the cylinder are used to connect a high-voltage supply to the PMT and for the output signal of the detector.

B. Radiation Localisation and Imaging

Up to four sensors can be coupled simultaneously to the MFA to measure neutron and/or γ radiation; in this paper we have focused on the γ radiation response. For example, in an inspection scenario, three channels could be used to provide uncollimated radiation intensity information in fixed directions, with the imaging setup utilizing a single sensor to provide more insight into areas of interest, e.g., entrance points, areas of unusually/unexpectedly high radiation intensity. A single sensor for the latter function has been applied in this research.

In a mobile radiation inspection scenario, the system constraints on power and size/mass payload can render bulky, multiple-sensor imaging systems designs impractical, whereas single-sensor alternatives can offer localization and imaging capabilities without compromising the critical
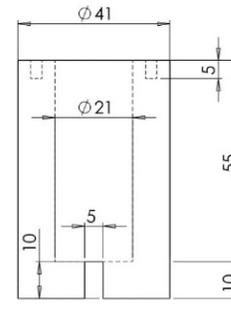

Fig. 4.   Plan view of lead collimator drawing.

operational functions of a robotic platform that they are coupled to.

The use of a single-sensor imaging configuration is also beneficial in stand-off situations where physical access to radiation environments may be a limiting factor. For instance, at Sellafield in the UK, narrow (6"/150 mm) ports are quite common initial points of access in facilities that have been closed for an extended period of time [20]. The system described in this article comprises such suitable equipment, by integrating servo-motors coupled to a collimated CeBr$_3$ detector. Slot collimators have been in use for many decades [21]–[26]. Their primary distinction from pinhole collimators is that the exposed detection surface of a slot is larger, and hence the probability of radiation interaction is greater, albeit with decreased spatial resolution. The strip-related spatial response can also enable regions of interest to be identified more rapidly by dedicated processing algorithms. Conversely, a pinhole collimator might require more scanning time which, in a mobile inspection scenario, might reduce battery life and implicate the limit of detection that is achievable.

The imaging setup developed for this research comprises a slot collimator made from lead, which surrounds the CeBr$_3$ detector. Dedicated servo motors have been configured to enable its field of view to be adjusted in terms of yaw, pitch, and rotation around its own axis (roll). Such systems have been tested previously (in stand-off mode) with success in radioactive environments (see e.g., [27], [28]). Fig. 4 shows side elevation and plan diagrams of the collimator. Its outer and inner diameters are 41 mm and 21 mm, respectively, resulting in 10-mm thick lead shielding around the detector. Its length is 65 mm with 10 mm partly covering the detection crystal via a 5-mm wide slit aperture. The exposed area of the surface of the detector casing can be approximated by a rectangle, 21 mm long and 5 mm wide. The collimator is finished with white paint to prevent any transfer of the material to people handling it. Lead was selected for its well-known attenuation characteristics, relatively low cost and ease of manufacture (particularly with respect to tungsten). However, in environments where lead is not preferred then tungsten would be a suitable alternative.

Monte Carlo simulations, performed with the tool MCNP6 [29], were used to calculate the attenuation reduction with 10 mm of lead for γ rays with energies consistent with those that can be derived from a range of isotopic sources and
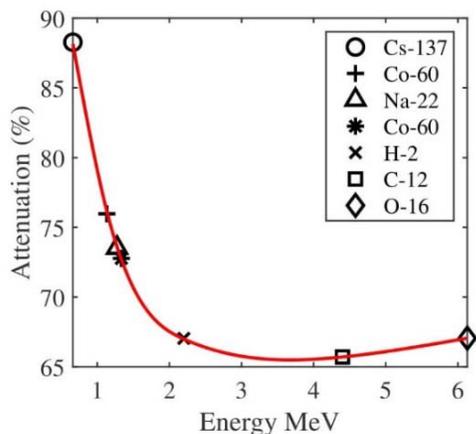
Fig. 5. γ-ray attenuation, in terms of % of incident γ-ray flux on lead against γ-ray energy (MeV), which is produced by nuclides (^{137}Cs, ^{60}Co, ^{22}Na), emitted following neutron capture on hydrogen, and neutron activation due to inelastic scattering (c.f., ^{12}C, ^{16}O).
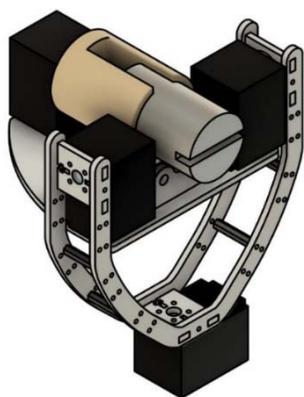

Fig. 6. A diagram, in perspective, of the gimbal design developed in this research including the slot collimator at its centre.

which can be present in nuclear environments, due to either radioactive isotopes or neutron-induced reactions. As depicted in Fig. 5, the attenuation is roughly 90 % for γ rays of approximately 0.6 MeV, and between 80 % and 65 % for energies of 1 MeV and above.

Fig. 6 depicts an isometric 3D drawing of the imager developed and tested in this research. Four Dynamixel (MX-28 AT) (www.robotis.us) actuators provide rotation of the collimator in the three principal axes. The bottom and two middle motors provide rotation on the pan (yaw) and tilt (pitch) axes, respectively, whilst the motor coupled to the collimator allows rotation (roll) around its axis of symmetry. A typical scanning routine involves rotating two of three axes, and reconstruction by means of iterative algorithms is essential to uncover the radiation distribution of a target area.

C. Overview of Operation and Integration With ROS

The Robot Operating System (ROS) is an open source middleware, equipped with tools and libraries that allow the development of custom robot applications [30]. Over the past decade, its utilisation has had a wide-reaching impact on the robotics community, in terms of user-friendliness,
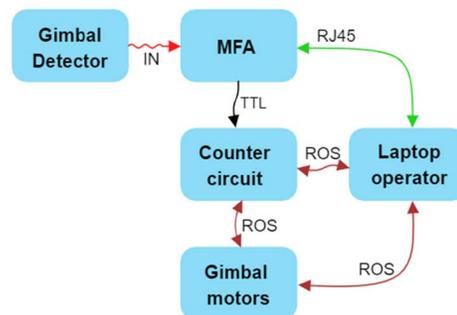

Fig. 7. Operation flow in a stand-alone inspection scenario.

and is now ubiquitous amongst robotic platforms. A novel feature of the instrumentation built for this research is that the radiation detection data acquisition hardware is straightforward to incorporate to robotic platforms that are ROS compatible. This enables direct control of the instrument by a robotic system and remote transmission of data back to the operator, while maintaining a low computational payload. Configurations local to the MFA can still be defined and output signals are transmitted via ROS. ROS can also be used when the instrumentation is in stand-alone mode, thus eliminating the need for an operator to reconfigure a different setup or different procedures. This is of particular interest in legacy environments where planning and regulatory approvals can be heavily reliant on the consistency of a given instrument with operating standards and protocols.

Fig. 7 depicts the operation of the apparatus with the imager in stand-alone mode. The first part involves the radiation detector coupled to the gimbal shown in Fig. 6 and the MFA. Via an Ethernet connection, configuration settings such as amplitude threshold and amplifier gain can be defined.

During operation, spectroscopic information is conveyed continuously to the laptop via the MFA's dedicated software. In parallel, its TTL output signal is fed to a four-channel, custom counter circuit. The latter comprises ubiquitous, small footprint microcontrollers (Teensy 3.2) that are configured to count radiation events on-demand or continuously. Communication with ROS is enabled within the code, so that data can be accessed in real time via the main ROS environment on the operator's laptop.

During a raster scanning routine, the ROS environment on the laptop calls a so-called node (written in the python^{TM} programming language) that invokes the motors to move sequentially to a set of orientations. Every time the motors reach their pre-specified location, they publish a unique flag which enables the counter circuit to accumulate radiation count events for a preset time period. In turn, the sum of radiation events is transmitted to the operator and the motors are instructed to their next position. When a radiation sensor is used without the gimbal, the counter circuit is simply instructed to accumulate radiation count events on-demand or continuously.

As is illustrated in the operational flow diagram in Fig. 8, migrating the stand-alone operation to a mobile inspection scenario is a straightforward task. The instrumentation is
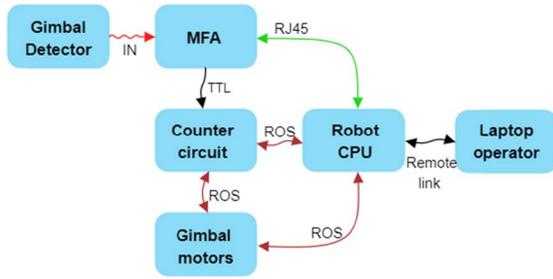
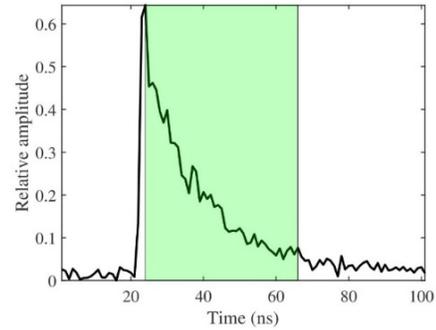Fig. 8. Operation flow in a mobile inspection scenario.

Fig. 9. Example output signal of a CeBr$_3$ detector, as a function of relative amplitude versus time, where the highlighted area indicates the time frame for which the integral is calculated.
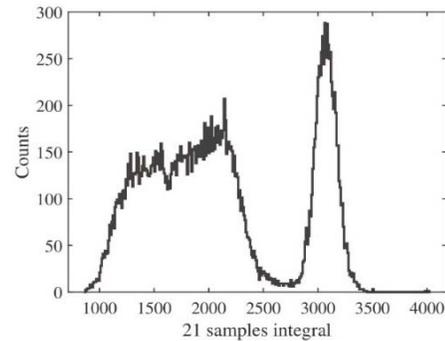

Fig. 10. An example spectrum from a sealed 307 kBq ^{137}Cs source recorded in this research, as a function of counts versus integral samples.

mounted on the robot platform and connected to the robot's CPU without the need to carry out custom-code modifications, and its operation control can be undertaken via a laptop with remote access to the robot's CPU.

The hardware presented in this section comprises an electronics box that houses the MFA, the custom ROS-enabled counter board, and a custom power supply distribution unit. The latter is powered by a 12 V DC connection and draws a current of approximately 1.8 A. A linear voltage regulator provides 7 V DC to the MFA and 5 V DC to the counter circuit. Dedicated high-voltage power supply modules (Hamamatsu C10940-03) are employed to power the radiation sensor, in static or variable mode, and can be switched on/off and specified on-demand via ROS. In variable mode, an additional microcontroller is coupled to a digital potentiometer, and in series with the high voltage module. The high voltage modules are characterised by high stability, and negligible measured voltage drift over long hour periods (standard deviation $\sigma = 0.0675$ V), which in turn ensures the stable performance of the PMT coupled to the radiation sensor.

III. RESULTS

A. Laboratory Results

One characteristic of the MFA is that its technology is compatible with fast scintillation detectors. The CeBr$_3$ used in this research yields fast timing pulses compatible with the hardware: mean rise and fall times of 1.5 ns and 35 ns, respectively. The MFA uses a pile-up rejection algorithm to ensure that the processed pulses are noise free, and in turn that the resulting spectral information is not distorted. Furthermore, its interface allows the specification of a trigger threshold above which a signal will be processed as a valid radiation event. This is commonly set two orders of magnitude higher than the mean detector signal baseline. Fig. 9 depicts a typical (normalised) signal response of the detector. Pulse-height spectroscopy is carried out by summing 21 sample amplitudes (42 ns) past the peak of the pulse (the area highlighted in green). The spectral information is thus conveyed by means of an integral, which is saved into an ASCII file for post-processing. A histogram can be then produced to constitute the fingerprint of γ-emitting radiation sources. Fig. 10 shows the resulting spectrum in the presence of a sealed 307 kBq caesium-137 (^{137}Cs) source.

The task of radiation imaging is a two-step process as the raw data retrieved from the collimated sensor have to be conditioned to produce the data that constitute a coherent distribution image. In this context, the former is a vector that contains the sum of radiation count events for a sequential set of measurement positions (D). The imager has been designed such that it can be adjusted, incrementally, in the following planes: horizontal (pan angle, p), vertical (tilt angle, t), and rotational (roll angle, r). During a scanning routine, data are obtained typically for a combination of pan and roll angles (p, r) at a single fixed tilt angle. The data acquisition duration is known *a priori* by multiplying p, r, and measurement time. It can vary depending on the conditions by which the instrumentation is used; primarily in terms of power capacity (battery powered when used on robots) and desired angular resolution, as well as distance from the target area.

The data vector is used, in turn, in a ubiquitous iterative reconstruction algorithm (Algebraic Reconstruction Technique). The estimated solution is computed using the following formula,

$$X^{k+1} = X^k + \lambda \frac{d_i - W_{pr}X^k}{\|W_{pr}\|^2} W_{pr} \qquad (1)$$

For each datum d_i in D, there exists a corresponding sensitivity distribution of the imager, W_{pr}. This is used as a weighting component in the algorithm and is a representation of the imager's viewpoint at a given measurement orientation. Vector X is the image solution updated in each iteration, whilst λ is a parameter that influences the speed with which the algorithm converges to a solution.
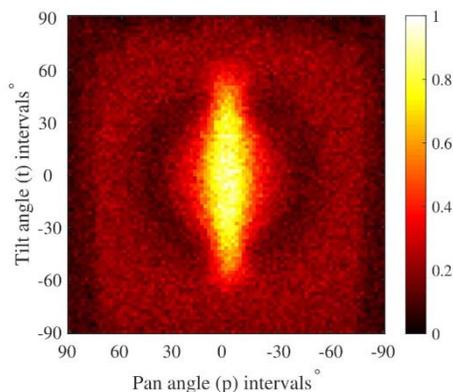
Fig. 11. Imager weighting matrix presented in terms of tilt angle interval versus pan angle interval.

Fig. 13. a) Experimental setup for the study of two point ^{137}Cs sources separated by 20 cm, showing gimbal-detector apparatus in the foreground and source arrangement in the background. b) Scanned data as a function of rotation angle versus pan angle, and c) A reconstructed image of two ^{137}Cs sources, in terms of vertical field of view versus horizontal field of view.
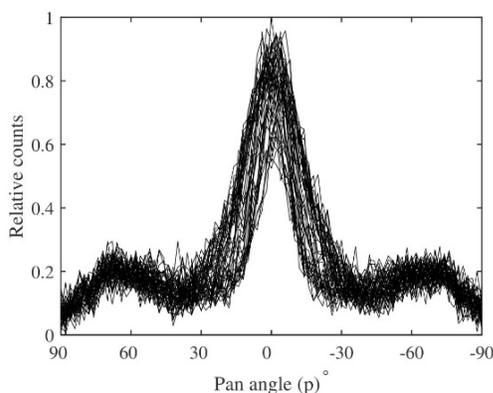

Fig. 12. Imager angle sensitivity: counts expressed relative to the maximum detected at a pan angle of 0° (collinear with the collimator), for tilt angles between −60° and 60°.

Fig. 14. An aerial view of the reactor hall showing the robot targeting the thermal irradiation port.

The sensitivity distribution matrix W was obtained experimentally: the imaging apparatus was rotated along the horizontal and vertical planes (−90° to 90°), with 2° intervals, and with the rotation angle fixed to 0° (vertical slot). A ^{137}Cs point source was placed across the detector-collimator at a centre position (corresponding pan and tilt angles $p = t = 0°$). Fig. 11 displays the resulting matrix, which can be then accordingly rotated and translated in the algorithm to reflect the collimated detector's position for each datum in D. The final reconstructed image solution (X) is mapped on the basis of the sensitivity matrix's size field of view (typically 180° in both vertical and horizontal planes), and useful vertical field of view of approximately 120°. The latter's corresponding scans through the horizontal plane are shown in Fig. 12, and indicate a mean 13° Full Width Half Maximum (17° for $p = t = 0°$).

As an example, two 307 kBq ^{137}Cs sources were placed diagonally and separated from each other by 20 cm, and the imager was placed 20 cm distant from the vertical plane shared by the sources. A scan comprised a set of 37 rotations of the roll angle and 19 rotations of the pan angle (5° intervals), totaling a 180° × 90° scan (703 discrete measurements). The overall duration of the data acquisition was 1.95 hours. Fig. 13a shows a picture of the experimental setup, with the instrumentation-imager in stand-alone mode targeting the two radioactive source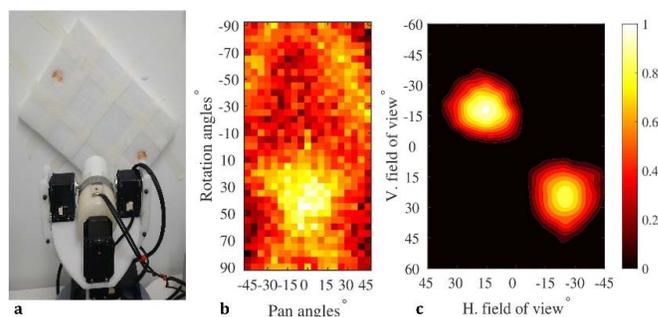s mounted on the wall. The raw data are presented in Fig. 13b, in which it can be observed that direct interpretation is not immediately possible. The reconstruction algorithm, solved to convergence, uncovers the actual distribution. As shown in Fig. 13c, the two sources are resolved, while their relative location in space is accurately captured by the imager.

B. Deployment at JSI TRIGA Mark II Reactor

The radiation imaging/spectroscopy system was tested both with a Jackal mobile robotic platform, and as a stand-alone instrument, at the JSI TRIGA Mark II reactor in Slovenia. This research reactor has a variety of uses, including neutron irradiation experiments [31], training and, of relevance to this research, it can also be used for γ irradiation purposes especially where a dispersed form of γ radiation (in terms of space and energy) is desirable for comparison with point-source responses: the energies of γ rays emitted by the reactor reach 10 MeV and above [32].

Fig. 14 shows the robot targeting the thermal irradiation port, which emits thermal neutrons and collimated γ radiation when the reactor is operating. Although not shown in this photograph, paraffin blocks were used in front of the collimated port to act as scatterers. Pulse height spectroscopy and imaging were carried out simultaneously, for 1.95 hours.

Fig. 15 shows a spectrum obtained from these measurements based on 100,000 total counts, with the peak around an integral value of 1750 corresponding to the 511 keV γ-ray peak due to electron-positron annihilation. Fig. 16 depicts the radiation distribution emitted from the thermal
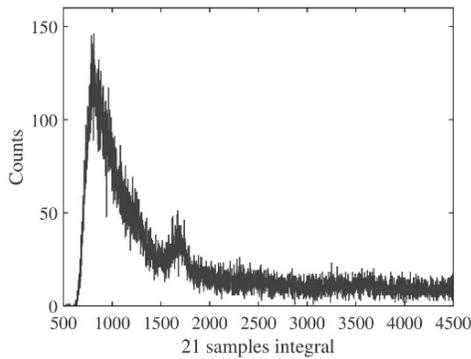
Fig. 15. A γ-ray spectrum taken at the thermal irradiation beamport of the JSI reactor.
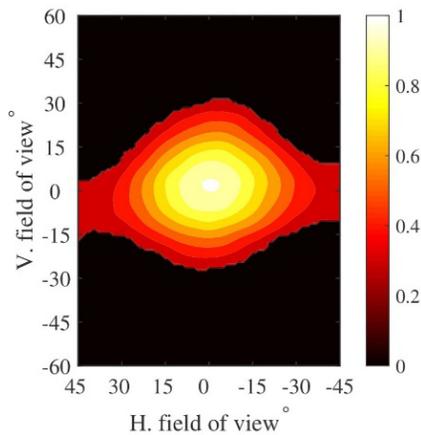

Fig. 16. A reconstructed γ-ray image of the thermal beamport, with the reactor operating at 1 kW.

Fig. 17. Stand-off radiation imaging on the reactor platform showing the instrument developed in this research and the reactor pool.

irradiation beamport. The raw data were collected, as previously, on the basis of a 5° interval, 180° × 90° scan of the roll and pan angle, respectively. Note that the image reconstruction is based on the corresponding spectral information, i.e., it is not tailored to a particular range of energies.

The instrumentation was placed, separated from the robot platform, on top of the reactor platform, to the side of the 2-m diameter pool (shown in Fig. 17) with the reactor operating at 75 kW. Fig. 18 displays the corresponding γ-ray spectra obtained simultaneously with the imaging scan. Results from approximately 400,000 pulses show again the 511 keV peak of annihilation radiation, whilst the peak on the right end may
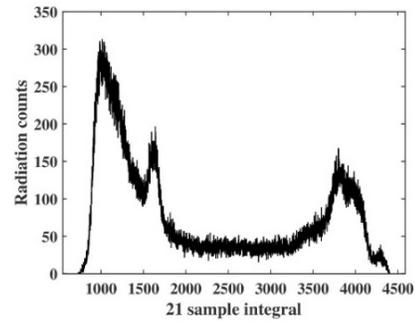

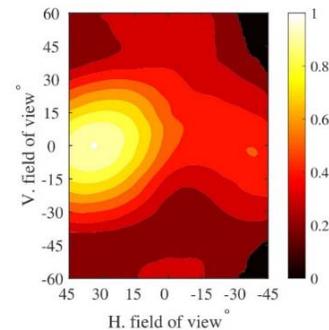Fig. 18. A γ-ray spectrum taken from the reactor platform.

Fig. 19. A reconstructed γ-ray image of the pool, with the reactor operating at 75 kW.

correspond to prompt γ-rays emitted directly from the core (with a mean energy of 2.5 MeV) and 2.2 MeV γ-rays arising from neutron-capture reactions on hydrogen.

The imager was fixed at a tilt angle of −45° (hence looking down towards the pool ring) and the scanning involved again 37 rotations of the roll angle and 19 rotations of the pan angle (5° intervals, 180° × 90° scan). The total duration for 5 s in each measurement position was 58 min. The initial pan angle implies that the collimated sensor is looking away from the reactor pool ring, to the right. The corresponding reconstruction (Fig. 19) reflects this as the majority of radiation intensity originates on its left side. Artefacts present on the image influence the shape of the reconstructed source and are partially due to the vicinity of the imager to the source. Despite these artefacts, a broad degree of localisation was possible.

IV. DISCUSSION

The instrumentation presented in this article appeals to the requirement of inspecting radiation facilities, and offers the capability to perform γ-radiation imaging and spectroscopy, simultaneously. It has been designed to be compatible with the need to access hard-to-reach areas, whilst provisions for ROS communication simplify its integration with mobile robotic platforms. This modular approach is particularly useful where time constraints apply in nuclear facilities, in terms of access, demand quick set-up times.

Its capability is further extended when used with a robotic platform, as multiple locations can be assessed without intervention by an operator to transfer it from place to place. The signal processing hardware can be exploited by employing

different sensors to indicate vicinity to unknown radiation fields and imaging can be then applied to areas of interest. In this research, the results were based on capability to detect γ radiation of up to 2.5 MeV. However, neutron detectors can be also coupled to identical hardware, given they have a similar form factor (such as those based on the EJ-301 scintillant used on backscatter measurements reported recently [33]). This exchange between different types of size-compatible sensors and, in turn, for discerning neutron and γ radiations, optimizes the amount of information that might be made available, and opens up its use to the monitoring of nuclear materials in forensics, security and safeguards applications.

The collimation for the purposes of radiation imaging is based on 10 mm of lead, which stops the majority (approximately 70 %) of γ-rays below 2 MeV. Therefore, the slit provides collimation, whereas the 10-mm thick lead shields the rest of the sensitive volume of the detector, thus reducing the number of γ-rays coming from directions beyond the field of view of the slit: more lead could be used but this would increase the payload of the instrumentation; using less lead would reduce the effectiveness of the collimator and would also degrade the signal/noise ratio (bias detector shielding). By virtue of the MCNP6 simulations, it was concluded that a thickness of 10 mm is an effective compromise in terms of balancing weight, cost and collimator/shielding requirements.

The ability to perform γ-ray spectroscopy and imaging in a reactor environment has been demonstrated. The reconstruction of images is carried out by a ubiquitous algorithm. Although the collimator sensitivity map was derived experimentally, and the scanning resolution is relatively low (5° intervals), the reconstructed images depict the location and distribution of radiation accurately in a spherical plane mapped to 2-dimensional coordinates. Hence, the amount of time allocated in imaging can be varied on the basis of desired resolution and number tasks and locations covered per mission.

The deployment at the JSI reactor represents a situation where a real-world, stable environment is inspected. Radiation levels in *ad-hoc* locations are often measured by workers, where the risk of exposure is deemed to be as low as reasonably practicable, or by remote means otherwise. Hence, coupling the radiation detection system to a robotic platform could replace this requirement and increase the resolution and consistency of information obtained. The results presented in this work show, as expected in this case, that operation of the reactor was normal since no contamination was detected. If the opposite had been the case, closer examination could have been undertaken using the same apparatus, whilst avoiding radiation worker exposure and with the advantage that assessments might be repeated and dwell times increased, in-situ, without routine recourse to safety cases and revised descriptions of work. It is worthy of note that such a scenario, based on a commercial robotic platform, avoids the significant cost and reliability issues that have plagued many robotic developments for nuclear legacy applications.

Finally, imaging scans have been carried out for a minimum distance of 20 cm (laboratory) and a maximum distance of 3 m (JSI). The reconstruction in a laboratory setting showed that it is possible to resolve two point sources at 20 cm, however,

measurements in more complex scenarios along this range will increase confidence with regard to the limits of this imager.

V. CONCLUSION

This article describes the design and commissioning tests of a small-footprint, portable radiation detection instrumentation system that can provide γ-ray spectroscopy and imaging information, simultaneously, and which can be incorporated easily to ROS-controlled robotic platforms. Its individual off-the-shelf and custom components are described and the results are presented on the basis of both laboratory and real-world settings, in this case in the vicinity of an operating reactor. As a research tool, the instrumentation can be modified to accommodate measurements using different detectors and imaging apparatuses. The incorporation of such technology in nuclear facilities could be a significant aid to routine inspections and potentially enable inspection of poorly understood legacies where the risk of exposure would otherwise prevent access.

REFERENCES

[1] World Nuclear Association. (2020). *Reactor Database*. Accessed: May 29, 2020. [Online]. Available: https://www.world-nuclear.org/information-library/facts-and-figures/reactor-database.aspx

[2] I. Tsitsimpelis, C. J. Taylor, B. Lennox, and M. J. Joyce, "A review of ground-based robotic systems for the characterization of nuclear environments," *Prog. Nucl. Energy*, vol. 111, pp. 109–124, Mar. 2019.

[3] M. Friedrich *et al.*, "Miniature mobile sensor platforms for condition monitoring of structures," *IEEE Sensors J.*, vol. 9, no. 11, pp. 1439–1448, Nov. 2009.

[4] H. Ishida, Y. Wada, and H. Matsukura, "Chemical sensing in robotic applications: A review," *IEEE Sensors J.*, vol. 12, no. 11, pp. 3163–3173, Nov. 2012.

[5] C. Ducros *et al.*, "RICA: A tracked robot for sampling and radiological characterization in the nuclear field," *J. Field Robot.*, vol. 34, no. 3, pp. 583–599, May 2017.

[6] B. Bird *et al.*, "A robot to monitor nuclear facilities: Using autonomous radiation-monitoring assistance to reduce risk and cost," *IEEE Robot. Autom. Mag.*, vol. 26, no. 1, pp. 35–43, Mar. 2019.

[7] Y. Xing *et al.*, "FireNose on mobile robot in harsh environments," *IEEE Sensors J.*, vol. 19, no. 24, pp. 12418–12431, Dec. 2019.

[8] L. Song, H. Wang, and P. Chen, "Automatic patrol and inspection method for machinery diagnosis robot—sound signal-based fuzzy search approach," *IEEE Sensors J.*, vol. 20, no. 15, pp. 8276–8286, Aug. 2020.

[9] *NDA Annual Report & Accounts*, Nucl. Decommissioning Authority, Cumbria, U.K., Dec. 2019.

[10] Y. Sato, Y. Terasaka, W. Utsugi, H. Kikuchi, H. Kiyooka, and T. Torii, "Radiation imaging using a compact Compton camera mounted on a crawler robot inside reactor buildings of Fukushima Daiichi nuclear power station," *J. Nucl. Sci. Technol.*, vol. 56, pp. 801–808, Oct. 2019.

[11] K. Vetter, R. Barnowksi, A. Haefner, T. H. Y. Joshi, R. Pavlovsky, and B. J. Quiter, "Gamma-ray imaging for nuclear security and safety: Towards 3-D gamma-ray vision," *Nucl. Instrum. Methods Phys. Res. A, Accel. Spectrom. Detect. Assoc. Equip.*, vol. 878, no. May 2017, pp. 159–168, 2018.

[12] M. J. Joyce, K. A. A. Gamage, M. D. Aspinall, F. D. Cave, and A. Lavietes, "Real-time, fast neutron coincidence assay of plutonium with a 4-channel multiplexed analyzer and organic scintillators," *IEEE Trans. Nucl. Sci.*, vol. 61, no. 3, pp. 1340–1348, Jun. 2014.

[13] M. D. Aspinall, M. J. Joyce, F. D. Cave, R. Plenteda, and A. Tomanin, "Automated response matching for organic scintillation detector arrays," *Nucl. Instrum. Methods Phys. Res. A, Accel. Spectrom. Detect. Assoc. Equip.*, vol. 861, pp. 46–54, Jul. 2017.

[14] M. Licata *et al.*, "Depicting corrosion-born defects in pipelines with combined neutron/γ ray backscatter: A biomimetic approach," *Sci. Rep.*, vol. 10, no. 1, pp. 1–11, Dec. 2020.

[15] SCIONIX. *Scintillation Detectors*. Accessed: May 29, 2020. [Online]. Available: https://scionix.nl/scintillation-detectors

[16] J. Caunt. *Cerium Bromide*. Accessed: May 29, 2020. [Online]. Available: https://johncaunt.com/materials/cebr3/

[17] A. R. Jones *et al.*, "On the design of a remotely-deployed detection system for reactor assessment at Fukushima Daiichi," in *Proc. IEEE Nucl. Sci. Symp., Med. Imag. Conf. Room-Temp. Semiconductor Detect. Workshop (NSS/MIC/RTSD)*, Oct. 2016, pp. 1–4.

[18] M. Nancekievill *et al.*, "Detection of simulated Fukushima Daichii fuel debris using a remotely operated vehicle at the Naraha test facility," *Sensors (Switzerland)*, vol. 19, no. 20, pp. 1–16, 2019.

[19] M. Nancekievill *et al.*, "Development of a radiological characterization submersible ROV for use at Fukushima Daiichi," *IEEE Trans. Nucl. Sci.*, vol. 65, no. 9, pp. 2565–2572, Sep. 2018.

[20] *Technology Development and Delivery Summary 2017-2018*, Sellafield, Sellafield, U.K., 2018.

[21] T. A. Tanaka and E. Iinuma, "Image processing for coded aperture imaging and an attempt at rotating slit imaging," in *Proc. 4th Int. Conf. Inf. Process. Scintigraphy*, 1975, pp. 43–55.

[22] G. R. Gindi *et al.*, "Imaging with rotating slit apertures and rotating collimators," *Med. Phys.*, vol. 9, no. 3, pp. 324–339, May 1982.

[23] S. Webb, M. A. Flower, and R. J. Ott, "Geometric efficiency of a rotating slit-collimator for improved planar gamma-camera imaging," *Phys. Med. Biol.*, vol. 38, no. 5, pp. 627–638, May 1993.

[24] G. L. Zeng and D. Gagnon, "CdZnTe strip detector SPECT imaging with a slit collimator," *Phys. Med. Biol.*, vol. 49, no. 11, pp. 2257–2271, Jun. 2004.

[25] A. C. Sharma, T. G. Turkington, G. D. Tourassi, and C. E. Floyd, "Near-field high-energy spectroscopic gamma imaging using a rotation modulation collimator," *Nucl. Instrum. Methods Phys. Res. B, Beam Interact. Mater. At.*, vol. 266, no. 22, pp. 4938–4947, Nov. 2008.

[26] J. M. C. Nilsson, R. R. Finck, and C. L. Rääf, "A rotating-slit-collimator-based gamma radiation mapper," *J. Environ. Radioactivity*, vol. 177, pp. 225–232, Oct. 2017.

[27] M. P. Mellor, B. A. Shippen, and M. J. Joyce, "Efficient single-detector gamma imaging for civil nuclear inspection," in *Proc. IEEE Nucl. Sci. Symp. Med. Imag. Conf. Rec. (NSS/MIC)*, Oct. 2012, pp. 433–438.

[28] J. S. Beaumont, M. P. Mellor, M. Villa, and M. J. Joyce, "Imaging of an operational nuclear reactor," *Nature Commun.*, vol. 6, pp. 1–6, May 2015.

[29] C. J. Werner *et al.*, "MCNP version 6.2 release notes," Los Alamos Nat. Lab., Los Alamos, NM, USA, Tech. Rep. LA-UR-18-20808, Feb. 2018.

[30] A. Y. Quigley *et al.*, "ROS: An open-source robot operating system," in *Proc. ICRA Workshop Open Source Softw.*, 2009, p. 5.

[31] K. Ambrožič, G. Žerovnik, and L. Snoj, "Computational analysis of the dose rates at JSI TRIGA reactor irradiation facilities," *Appl. Radiat. Isot.*, vol. 130, pp. 140–152, Dec. 2017.

[32] L. Snoj *et al.*, "Radiation hardness studies and detector characterisation at the JSI TRIGA reactor," in *Proc. EPJ Web Conf.*, vol. 225, Jan. 2020, p. 04031.

[33] M. D. Aspinall *et al.*, "Real-time capabilities of a digital analyzer for mixed-field assay using scintillation detectors," *IEEE Trans. Nucl. Sci.*, vol. 64, no. 3, pp. 945–950, Mar. 2017.

Ioannis Tsitsimpelis received the Ph.D. degree in control engineering from Lancaster University, U.K. He is currently a Postdoctoral Research Associate with Lancaster University, carrying out research for the TORONE project. His research interests include data-based modeling and control, radiation detection, electronics, and digital signal processing.

Andrew West received the M.Phys. degree in physics with nanotechnology from the University of Leicester, and the Ph.D. degree from the University of York in Plasma Physics, before working as a Research Associate in compact X-ray lasers. He joined the University of Manchester Robotics for Extreme Environments Group as a Postdoctoral Research Associate in 2017. His research interests in robotics for nuclear decommissioning range from the integration of novel radiation and photonic sensing with robots to using autonomous behavior to improve data quality. His general research interests include experimental data analysis, robust error estimation, and instrument design.

Mauro Licata is currently pursuing the Ph.D. degree with Lancaster University. His research regards the development of a combined fast-neutron/gamma-ray computed tomography technique using an isotopic radiation source and a real-time detection system for both fast neutrons and gamma rays.

Michael D. Aspinall (Member, IEEE) received the Ph.D. degree from the Think Crime! EPSRC research project (EP/C008022/1), which formed the DISTINGUISH Consortium in 2008. His research began during his degree in mechatronic engineering in 2005, with contributions toward the design and implementation of an advanced neutron spectrometer funded by an EPSRC Instrumentation Development Award (GR/R38538/01). His work here specifically focused on real-time digital assay of mixed radiation fields with prominent developments in real-time, digital pulse-shape discrimination of neutrons, and gamma rays. Further extensive work led to the embodiment of these findings into technology with a TRL 9 that has served several nuclear establishments, supporting additional research in nuclear safeguards, non-proliferation, neutron imaging, and fast-neutron multiplicity analysis. Most notably, during his time in industry, he oversaw the delivery of the bespoke processing hardware and software for the ADRIANA liquid scintillator array at Lancaster University, as a part of the National Nuclear User Facility (NNUF) (EP/L025671/1). He currently holds the position of the International Senior Lecturer in Digital Electronics at Lancaster University. As a part of the TORONE Consortium, he is responsible for overseeing the ruggedized acquisition and analytical hardware and software implementations for the characterization of radioactive contaminants.

Anže Jazbec received the B.Sc. degree from the University of Ljubljana in 2012. Since then, he is employed by the Jožef Stefan Institute at TRIGA research reactor as a Reactor Operator and Operator of the Hot Cell Facility. In 2016, he became a supervisor. As an operator, he is strongly involved in administrative work such as the development of working procedures, performing various safety analyses and preparation of new experiments. In the field of research, he has about nine years of experience in MCNP calculations, which are mainly focused on TRIGA reactors.

Luka Snoj (Member, IEEE) received the Diploma and Ph.D. thesis in physics from the Faculty of Mathematics and Physics, University of Ljubljana, Slovenia, in 2005 and 2009, respectively. In 2010, he has been appointed as the Head of TRIGA Reactor at the Jožef Stefan Institute (JSI), where he has been the Head of the Reactor Physics Division since 2014. He is very active in teaching; reactor and radiation physics, experimental reactor physics at the Faculty of Mathematics and Physics, where he was an elected Associate Professor in 2019. He has been an advisor to nine master's and three Ph.D. theses and is an advisor to four Ph.D. students. His research interest is mainly in theoretical reactor physics related to practical applications in power and research reactors, in particular: Monte Carlo transport of neutrons and photons in fission and fusion nuclear reactors, integral reactor experiments, as well as criticality experiments and calculations. He regularly performs evaluations and evaluation reviews of critical and reactor physics experiments for International Criticality Safety Benchmark Evaluation Project (ICSBEP) and International Reactor Physics Experiment Evaluation (IRPhE) Project working groups under OECD/NEA.

Philip A. Martin received the first degree in chemistry from the University of Oxford and the Ph.D. degree in physical chemistry from the University of Cambridge. He is a Professor of Chemical Engineering with the Department of Chemical Engineering and Analytical Science, University of Manchester. His current research interests include the process analytical technology involving *in situ* and remote analysis in the process and nuclear industries and have published over 90 articles in international journals. He is the PI of the EPSRC-funded TORONE project. Recently, he has become a Fellow of the Royal Society of Chemistry and also a Fellow of the Institute of Physics. He founded the university spin-off company, TDL Sensors Ltd., which was recently sold to Envea.

Barry Lennox (Senior Member, IEEE) is a Fellow of the Royal Academy of Engineering and a Professor of Applied Control and Nuclear Engineering Decommissioning with The University of Manchester. He is also the Director of the Robotics and Artificial Intelligence for Nuclear (RAIN) Research Hub that received £12M of funding through the ISCF Robotics for a Safer World programme. RAIN has led to many first-of-a-kind robotic deployments, including CARMA, which became the first fully autonomous robot to be deployed into an active facility on the Sellafield site. Prof. Lennox also leads the £5M EPSRC Programme Grant: Robotics for Nuclear Environments, and the robotics work within various other projects, including the EPSRC TORONE project.

Malcolm J. Joyce (Member, IEEE) received the B.Sc. (Hons.) degree in physics, the Ph.D. degree in γ-ray spectroscopy, and the D.Eng. degree in digital fast neutron assay. He is currently a Professor of Nuclear Engineering at Lancaster University, U.K. His research interests include applied radiation detection and measurement, decommissioning-related analytical methods, and nuclear policy and environmental assay. He is an author of over 160 refereed journal articles and has specialized of late in digital mixed-field radiation assay with fast, organic liquid scintillation detectors. He is a member of the U.K. Government's Nuclear Industry Research Advisory Board (NIRAB) and is the Co-Chair of U.K.'s National Nuclear Users' Facility (www.nnuf.ac.uk). In 2014, his team was awarded the James Watt medal by the Institution of Civil Engineers (www.ice.org.uk) for best paper in the journal *Proceedings of Institution of Civil Engineers* (ICE) (Energy) for research on the depth profiling of radioactive contamination in concrete. In 2016, he was awarded a Royal Society Wolfson Research Merit Award. In 2017, he completed the monograph: *"Nuclear Engineering—A Conceptual Introduction to Nuclear Power."*